Space Mission Control: A Zero-Backend Browser Suite for Sun-to-Satellite Space-Weather Situational Awareness

Ka Wah Philip Ng
PhD, FCPA (Aust. & HK), FCMA, CESGA
Independent Researcher, Hong Kong
ngkwphilip@gmail.com · ORCID: 0009-0009-3955-010X

Abstract—Public space-weather and satellite-catalogue data are freely available, yet remain largely inaccessible to non-specialists: the telemetry is technical, the formats are brittle, and the operational meaning is rarely stated in plain language. This paper presents Space Mission Control, a suite of three self-contained, single-file web dashboards wrapped in a tab shell, which together reconstruct one causal chain — what the Sun is doing, what that does to the near-Earth space environment, and which orbiting objects feel the effect. Tab 1 monitors solar X-ray activity, NOAA R/S/G impact scales, and ten-channel NASA SDO imagery; Tab 2 converts live NOAA indices (Kp, F10.7, Dst, solar wind) into per-altitude-band orbital-drag impact through an empirical thermospheric-density model and a what-if calculator; Tab 3 propagates a deliberately sampled ~670-object CelesTrak catalogue with SGP4 on an interactive globe, including live three-dimensional proximity context around any selected object. All computation is client-side JavaScript; there is no backend, build step, account, or API key. We describe the architecture, the design principle of honest degradation under network blocking, practitioner lessons from migrating to CelesTrak's current gp.php API and rate-limit policy, and a case study of the August 8–15, 2026 geomagnetic-storm week. The suite is deployed as a static site and released under the MIT licence.

Index Terms—*space weather, orbital drag, satellite situational awareness, SGP4, TLE, CelesTrak, NOAA SWPC, NASA SDO, dashboard, decision support, zero-backend web application.*

I. Introduction

When the Sun erupts, the consequences arrive at Earth on two clocks: electromagnetic radiation within eight minutes, and coronal-mass-ejection plasma one to three days later. Both pump energy into the thermosphere, which expands; satellites in Low Earth Orbit (LEO) then experience increased atmospheric drag, decay faster, and — operationally most disruptive — drift away from their published orbit predictions. This chain is well understood scientifically, yet the public data describing it are scattered across specialised services whose output is intelligible mainly to practitioners: X-ray flux time series from NOAA's GOES satellites, geomagnetic indices (Kp, Dst), solar radio flux (F10.7), and Two-Line Element (TLE) catalogues.

Space Mission Control is a suite of three live web dashboards — a Solar Imagery Analyst, a Space Weather & Drag dashboard, and an Orbital Object Tracker — wrapped in a single tab shell in the order of the causal chain: the cause (the Sun), the near-Earth effect (space weather and thermospheric drag), and the population that feels it (the satellite fleet). The suite's distinguishing design choice is translation: each dashboard converts raw telemetry into plain-language, decision-oriented statements, such as "the illustrative model estimates ~47% higher relative drag for objects in the 400–500 km LEO band over the next 48 hours," generated by rule-based engines that mimic the output shape of a multimodal large language model at zero API cost.

The entire suite is zero-backend: each dashboard is a single self-contained HTML file (roughly 700–1,100 lines of HTML/CSS/vanilla JavaScript) that fetches public, CORS-enabled data directly in the viewer's browser. There is no server, database, authentication, or build step; deployment is a drag-and-drop of four files onto a static host. This paper describes the system (Sections III–VI), a case study of the geomagnetically active week of August 8–15, 2026 (Section VII), practitioner lessons that may benefit other builders of public-data tools (Section VIII), and limitations and future work (Sections IX–X).

The contributions of this work are threefold: (1) an integrated Sun-to-satellite browser workflow that connects solar imagery, space-weather indices, and the orbital population in a single static deployment; (2) a zero-backend architecture with explicit, honest degraded states under network blocking; and (3) plain-language translation of technical public telemetry for non-specialists. We do not claim algorithmic novelty: as Section X elaborates, the contribution is less any single algorithm than a set of working patterns.

II. Related Tools and Data Sources

The constituent data are public and authoritative. NOAA's Space Weather Prediction Center (SWPC) publishes JSON feeds for Kp, F10.7, Dst, solar wind, official alerts, and the R/S/G space-weather scales [1], [8]. NASA's Solar Dynamics Observatory (SDO) publishes near-live imagery in ten AIA/HMI channels [5]. CelesTrak publishes the public General Perturbations (GP) orbit catalogue as TLE and JSON/OMM element sets [2], and satellite.js provides a mature JavaScript implementation of the SGP4/SDP4 propagators [7], [3], [4].

General-purpose space-weather dashboards (e.g., SpaceWeatherLive) present indices and imagery but do not translate them into orbital-drag impact per altitude band. Catalogue trackers and conjunction services (CelesTrak, Space-Track, commercial SSA providers) track objects but do not connect live space weather to decay implications in plain language. The niche of the present suite is the join: one causal narrative from solar imagery to per-band relative-drag indicators to orbital objects selected for high drag sensitivity, in a single static deployment requiring no accounts.

III. System Architecture and Design Principles

A. Zero-backend static architecture

Each dashboard is one HTML file with at most two CDN dependencies (Chart.js; satellite.js). All data fetches are client-side against public CORS-enabled endpoints. The tab shell (Space_Mission_Control/index.html) embeds the three dashboards as lazy-loading iframes; once loaded, each tab stays alive so state persists while switching. Editing follows a single-source convention: each dashboard lives in its own folder and is copied into the shell folder after each change.

B. Rule-based translation engines

Each tab contains a rule-based three-part narrative engine that reads the current telemetry and emits a fixed three-part statement — what has happened, what is happening, what is likely to happen. The engines reproduce the output format a multimodal LLM call would produce, but run deterministically, offline-capable, at zero cost; the design anticipates a future upgrade in which the same panels are fed by a vision-language-model endpoint (Section IX).

C. Honest degradation

Public endpoints are routinely unreachable from corporate or filtered networks. Rather than rendering blanks or silently fabricating flat lines, every panel has an explicit degraded state: per-feed fallback values labelled "Demo data," a grey "Feed unavailable" panel state (Fig. 3), and diagnostic banners that name the failed feed and provide a one-click test link. We regard this honesty as a feature, not an apology: a situational-awareness tool that silently invents data is worse than no tool.

Table I. The three subsystems at a glance.

Component	Primary inputs	Processing	Main output
Solar Analyst (Tab 1)	GOES X-ray, NOAA R/S/G scales, SDO imagery	Rule-based interpretation	Solar-activity narrative
Space Weather & Drag (Tab 2)	Kp, F10.7, Dst, solar wind	Heuristic density/drag model	Relative drag impact by altitude band
Orbital Tracker (Tab 3)	CelesTrak GP data	SGP4 propagation	Object positions and proximity context

IV. Subsystem I — Solar Imagery Analyst (Tab 1)

Tab 1 answers "is the Sun quiet or erupting right now?" Its panels (Fig. 1) are: (i) the current GOES X-ray flare level on the logarithmic A/B/C/M/X class scale (each class ten times the previous); (ii) a 24-hour X-ray flux chart with class bands; (iii) NOAA's R/S/G impact scales (radio blackouts, solar radiation storms, geomagnetic storms), 0–5, with forecast probabilities where published; (iv) a latest-flare-events table; and (v) the rule-based three-part narrative. A ten-channel grid of near-live SDO images (Fig. 2) is loaded via plain image tags, which pass corporate proxies that block JSON APIs.

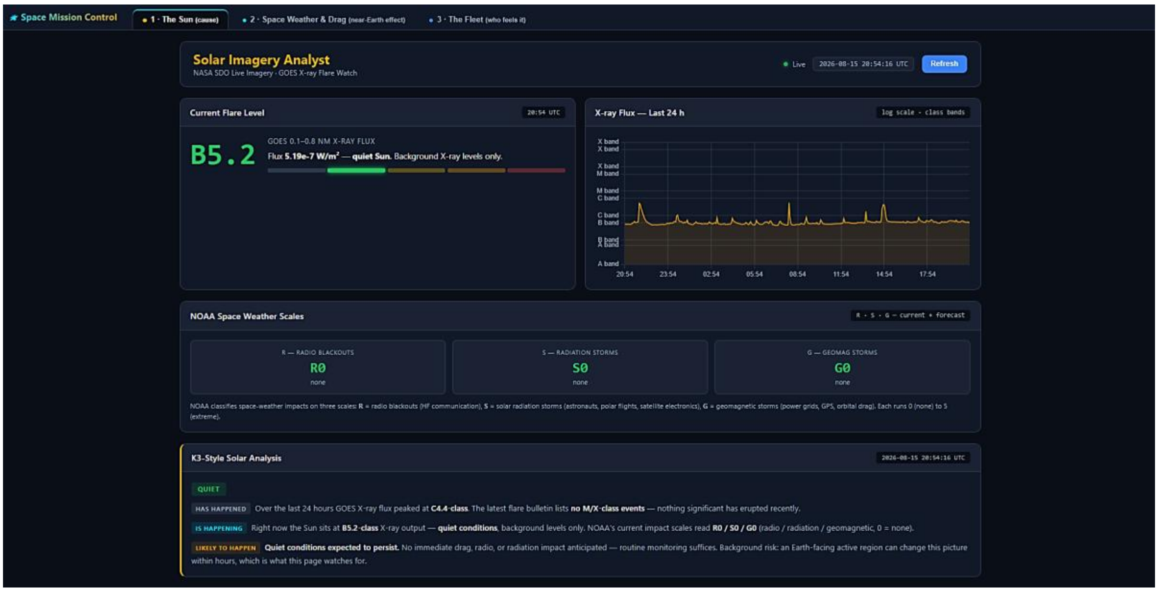

Fig. 1. The tab shell with Tab 1: current flare level (B5.2, quiet), 24-h GOES X-ray flux, NOAA R/S/G scales (all zero), and the rule-based three-part solar narrative. Captured 2026-08-15 20:54 UTC.

Fig. 2. "Sun Now": ten near-live NASA SDO channels (AIA 94–211 Å, 304 Å, 1600 Å, 1700 Å; HMI magnetogram and continuum), refreshing every 15 minutes.

V. Subsystem II — Space Weather & Drag (Tab 2)

A. Empirical density model

The dashboard ingests Kp, F10.7, Dst, and propagated solar-wind speed, and computes a thermospheric density multiplier relative to a quiet-Sun baseline (F10.7 = 70 sfu, Kp = 2, wind = 400 km/s, Dst = 0):

$$M = f(F10.7) \cdot f(Kp) \cdot f(SW) \cdot f(Dst)$$

with f(F10.7) = exp((F10.7 − 70)/200) (EUV-driven heating), f(Kp) = 1 + 0.12·max(0, Kp − 2) (Joule heating), f(SW) = 1 + 0.5·max(0, (SW − 400)/500), and f(Dst) = 1 + 0.3·max(0, −Dst)/100. Drag increase per altitude band is (M − 1) × 100% scaled by an altitude sensitivity (1.15 below 250 km, 1.0 for 250–500 km, 0.7 for 500–650 km, 0.4 above); decay in km uses a quiet-Sun baseline decay table scaled by M and the forecast window. Risk levels run LOW / MODERATE / HIGH / CRITICAL at 10 / 30 / 60% thresholds.

The coefficients are heuristic sensitivity parameters chosen to produce qualitatively plausible responses to changing space-weather conditions; they have not been calibrated against satellite-derived density measurements or validated against an operational thermospheric model. Accordingly, the resulting drag and decay values should be interpreted as illustrative relative-impact indicators rather than orbital predictions. A full thermospheric model such as NRLMSISE-00 [6] would provide a more physically grounded density estimate, but requires additional inputs and introduces complexity inconsistent with the suite's deliberately lightweight explanatory design; the present model therefore prioritises transparent, browser-native relative-impact estimation over operational density prediction. Integration of a validated atmospheric model is a natural future extension (Section IX).

B. Panels

Four metric cards with sparklines; a headline alert banner stating severity, drivers, affected bands, and the density multiplier in plain language; a switchable timeline chart (Fig. 4); five orbital-band impact cards giving drag increase and 7-/30-day decay per band (Fig. 5); a custom drag calculator for arbitrary what-if scenarios (Fig. 6); the official NOAA alerts feed; and an R/S/G scales panel. Fig. 3 shows the dashboard during a real partial outage on the authors' network: the solar-wind panel displays its honest "Feed unavailable" state while the model continues on the remaining live drivers plus a climatological wind estimate. Figures 3–8 are timestamped captures of the deployed interface during the case-study period; subsequent interface revisions use the more cautious terminology adopted in the manuscript, including "illustrative model estimate" and "heuristic re-entry band."

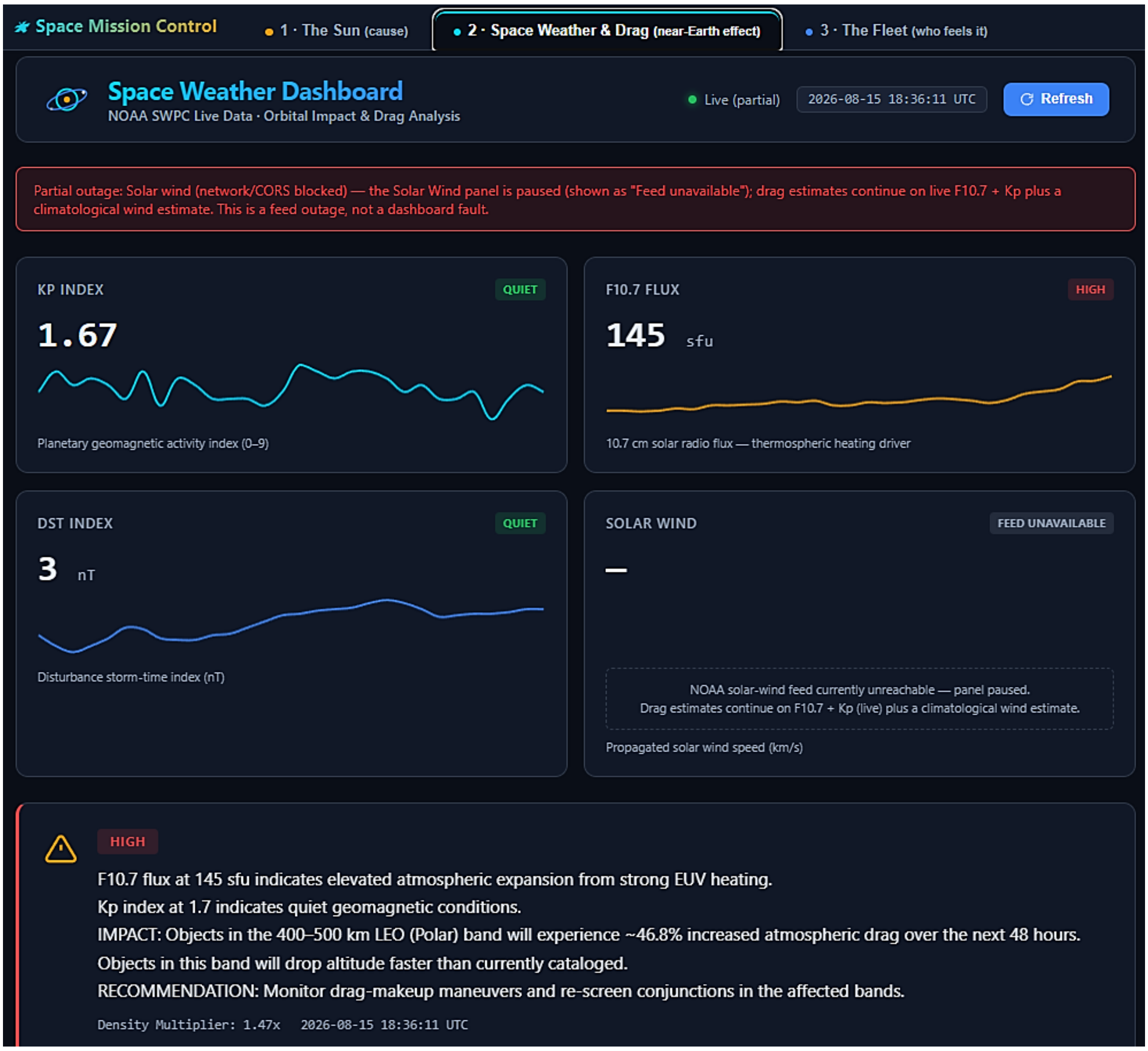

Fig. 3. Tab 2 during a genuine partial feed outage (2026-08-15 18:36 UTC): solar wind "Feed unavailable," drag model continuing on live Kp (1.67) and the feed's F10.7 value (145 sfu as displayed; the definitive observed value that day was 117 sfu — see Section VIII, item 7); alert banner reports a 1.47× density multiplier and ~46.8% drag increase for the 400–500 km band.

Fig. 4. Combined timeline, August 8–15, 2026: Kp × 10 (cyan), F10.7 (orange), Dst (blue). The August 8 geomagnetic storm is visible in the Kp and Dst traces. Note that the displayed F10.7 trace peaks near 215 sfu mid-week, whereas the definitive Penticton record shows a gentle rise from 94 to 117 sfu — a feed-content discrepancy documented in Section VIII, item 7.

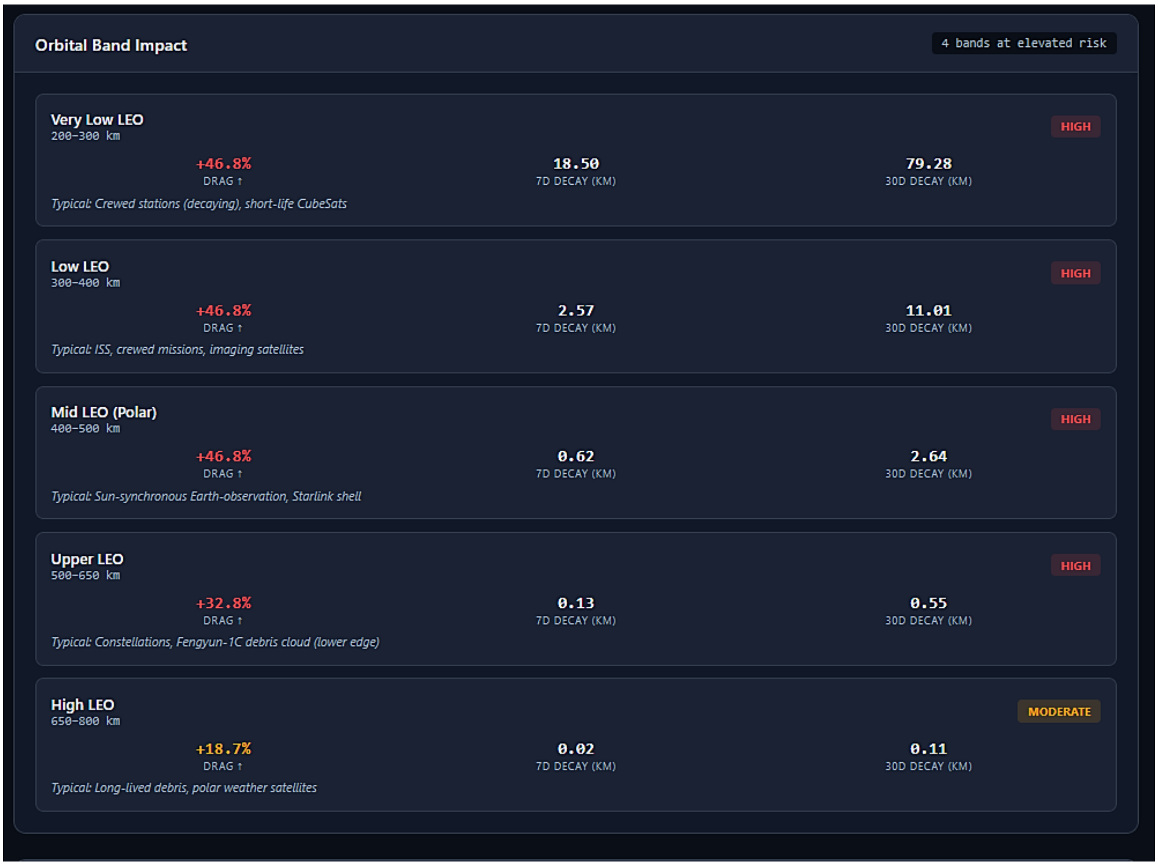

Fig. 5. Orbital Band Impact cards: drag increase and 7-/30-day decay for five LEO bands. At a 1.47× multiplier, the illustrative model projects ~18.5 km of 7-day decay at 200–300 km and ~0.6 km at 400–500 km.

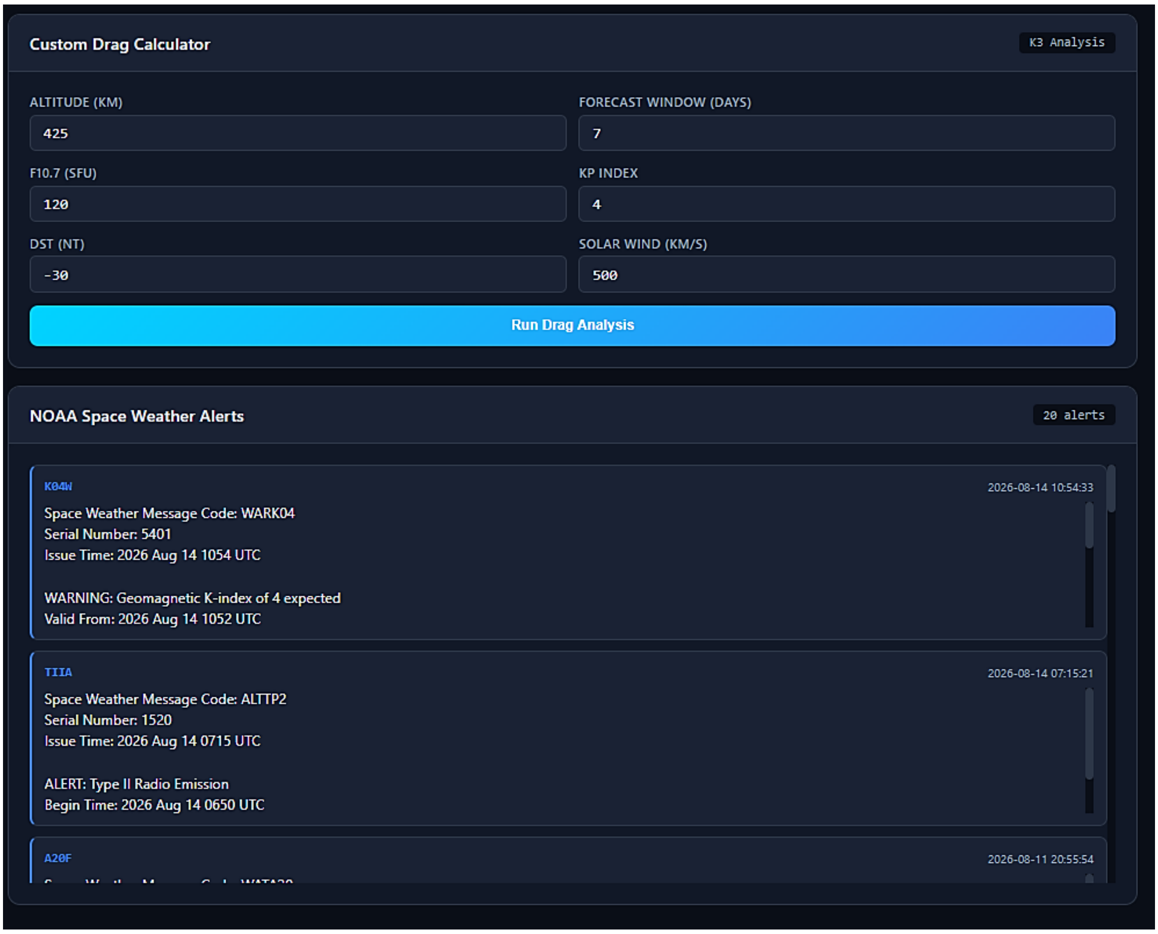

Fig. 6. Custom Drag Calculator (arbitrary altitude, window, and driver scenario) above the official NOAA SWPC alerts feed.

VI. Subsystem III — Orbital Object Tracker (Tab 3)

Tab 3 addresses the population question: which tracked objects are in orbit right now, and which are decaying fastest? From CelesTrak's gp.php API it loads four categories — stations (20), active satellites (300), high-drag debris (200), and rocket bodies (150) — and propagates every object with SGP4 onto a rotatable orthographic globe (Fig. 7), refreshed every 10 seconds. The debris sample is chosen, not incidental: the tracker fetches all ~15,000 catalogued debris objects by the NAME=DEB naming convention and keeps the 200 with the highest values of the TLE BSTAR drag parameter, used here as a heuristic indicator of drag sensitivity — the population most affected by the conditions modelled in Tab 2. An auto-generated Situation Brief (Fig. 7) recomputes the three-part narrative from the live catalogue on every load.

Interaction features include a name/NORAD search box, a clickable full catalogue list, a pulsing marker on the lowest object, an expand-globe mode, and live proximity context: selecting any object lists the tracked debris fragments and rocket bodies within 2,000 km in three-dimensional ECI distance, ringed on the globe with dashed circles (Fig. 8). The proximity display is a situational-visualisation feature, not a conjunction assessment: instantaneous separation between TLE-propagated positions does not represent probability of collision or predict time of closest approach, and no covariance, uncertainty, or screening-volume analysis is performed. The same caveat is displayed in the dashboard next to the feature.

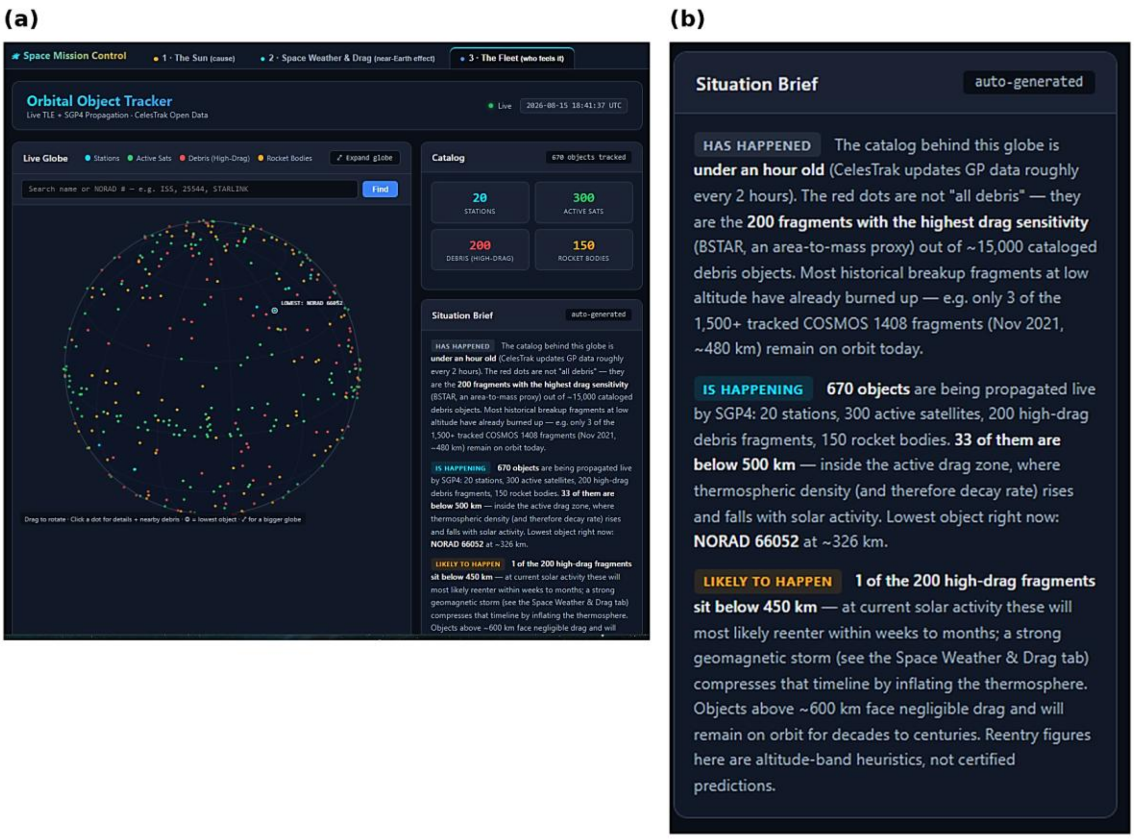

Fig. 7. Tab 3 overview (2026-08-15 18:41 UTC). (a) Main view: 670 objects propagated live — 20 stations, 300 active satellites, 200 high-drag debris, 150 rocket bodies — with catalogue summary; the lowest object (NORAD 66052, ~326 km) carries a pulsing marker. (b) The Situation Brief: has happened (catalogue age; what the BSTAR-ranked debris sample represents), is happening (counts; 33 objects below 500 km; lowest object), likely to happen (re-entry outlook; storm sensitivity).

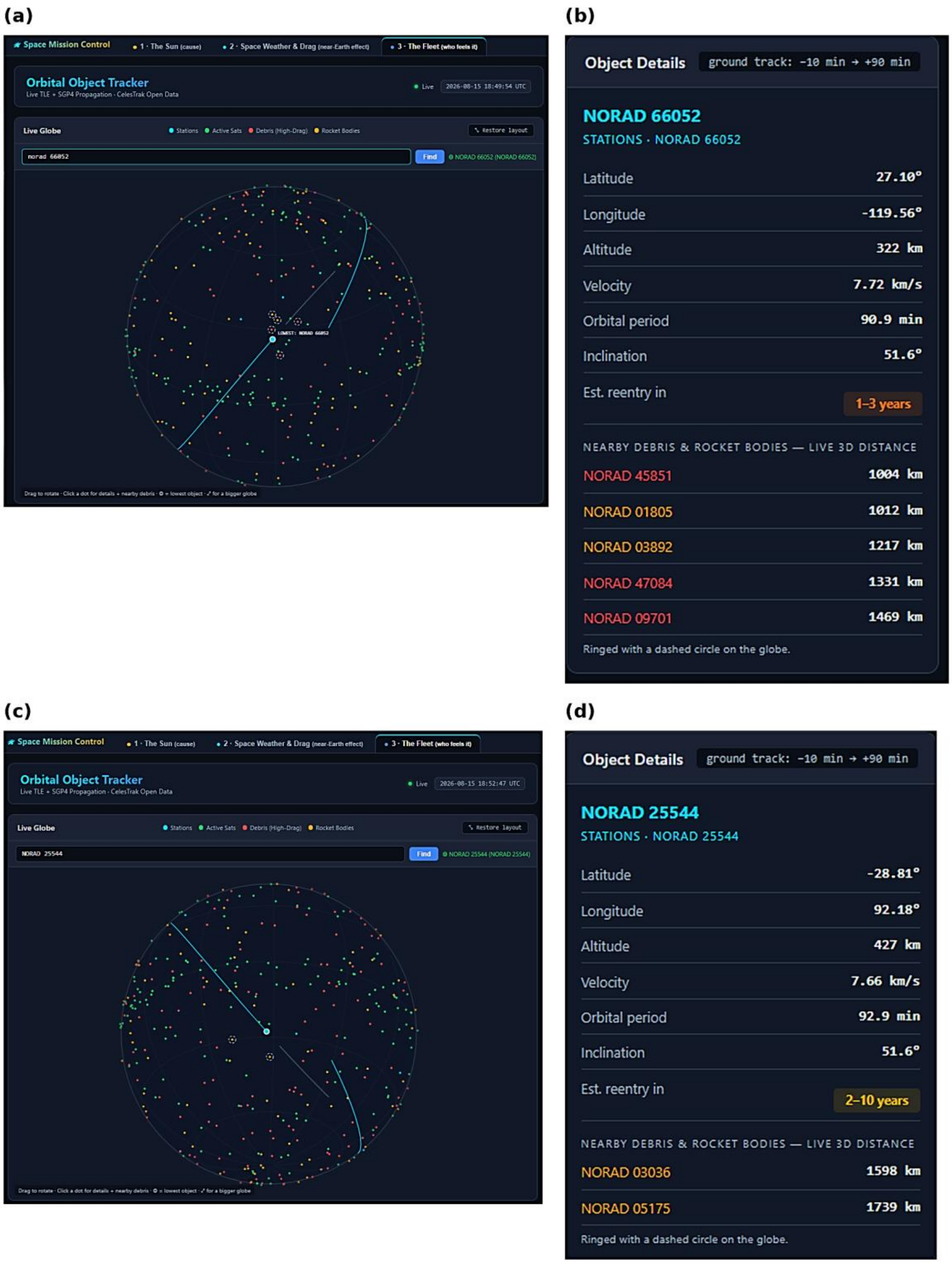

Fig. 8. Proximity context (situational visualisation, not conjunction assessment). (a, b) NORAD 66052 in expand-globe mode: dashed white rings mark tracked debris/rocket bodies within 2,000 km; the details panel lists them with live 3D distances (1,004–1,469 km), alongside position, velocity, period, inclination, and a heuristic re-entry band. (c, d) NORAD 25544 (ISS) located by search: globe rotated to the object with its 90-minute ground track (−10 min grey, +90 min coloured); details show two nearby tracked objects at 1,598 and 1,739 km.

VII. Case Study: The Week of August 8–15, 2026

The suite ran throughout an active space-weather week. On August 8, NOAA SWPC's estimated planetary Kp reached storm level (6; official ALTK06 alerts timestamped 21:00 UTC; the GFZ definitive Kp for the day peaked at 5.7) while the Kyoto Dst index fell to −60 nT — the classic Kp-up/Dst-down storm signature, visible in the timeline (Fig. 4). The definitive Penticton F10.7 record, by contrast, shows only a gentle rise over the week, from 94 sfu on August 8–9 to 117 sfu on August 15.

A worked example from the storm peak on August 8 (F10.7 ≈ 94 sfu, Kp ≈ 5.7, Dst = −60 nT, solar wind at its 400 km/s baseline): the model produced M ≈ 1.13 × 1.44 × 1.00 × 1.18 ≈ 1.9, i.e., ~+90% relative drag for full-sensitivity bands and ~0.8 km of model-projected 7-day decay at 450 km — nearly twice the quiet-Sun rate, driven by geomagnetic (Kp, Dst) rather than radiative (F10.7) forcing. By August 15 the geomagnetic field had quieted (Kp = 1.67, Dst = +3 nT) while the dashboard's F10.7 feed displayed 145 sfu — the definitive observed value that day was 117 sfu; the feed interleaves forecast entries, a parsing trap documented as Section VIII, item 7 — yielding M ≈ 1.47 as displayed (M ≈ 1.28 on the definitive value) and a chronic ~+47% relative drag at full-sensitivity bands: the post-storm "warm atmosphere" regime in which elevated thermospheric density can continue to affect orbital drag even when no storm warning is active.

Tab 3 supplied the population context for the same moment: 33 of 670 tracked objects below 500 km (inside the active drag zone), the lowest at ~326 km with a heuristic 1–3-year re-entry band, and — during the storm-free but elevated week — one of the 200 high-drag fragments already below 450 km. The proximity feature let a non-specialist answer "what is flying near the ISS right now?" in two clicks (Fig. 8). The causal chain was thus readable end-to-end from one tab shell: eruption watch (Tab 1) → modelled relative thermospheric-drag impact (Tab 2) → orbital-object context (Tab 3).

VIII. Lessons Learned

1) Public APIs change under you. CelesTrak retired its legacy bulk.php endpoint (now HTTP 404) in favour of gp.php; legacy GROUP names are not all valid gp.php groups, and invalid queries return an HTML information page rather than an error — parsers must reject non-data responses explicitly. The naming-convention queries NAME=DEB and NAME=R/B proved the robust replacement for retired debris/rocket-body groups.

2) Know your upstream format. gp.php TLE responses arrive as two-line TLEs with no name line, so list UIs fall back to "NORAD nnnnn" identifiers (visible in the catalogue panels); name-aware displays need the JSON/OMM variant.

3) Be a polite client. CelesTrak answers aggressive polling with HTTP 403 temporary IP blocks, and reloading during a block extends it. The tracker therefore sends one clean request per feed, paces feeds 1.5 s apart, stops immediately on 403, and refreshes on the provider's actual ~2-hour update cadence. Shared VPN exit IPs can be throttled by other users' traffic — worth documenting for users.

4) Rank populations, not individuals, with BSTAR. BSTAR is an empirical fitted coefficient — occasionally zero, negative, or noisy per object — but provides a convenient catalogue-scale heuristic for identifying objects whose fitted orbital solutions exhibit stronger drag-related effects; the 200-fragment sample should be read accordingly.

5) Plan for the 6-digit catalogue. The 5-digit catalogue number space was exhausted on 2026-07-11; objects numbered 100000+ have no TLE representation. TLE-first with JSON/OMM fallback (and satellite.json2satrec) is the durable path.

6) Honest degraded states preserve trust. Users tolerated — and screenshotted — the "Feed unavailable" panel; a fabricated flatline would have been discovered and remembered.

7) Feeds mix observations and forecasts — cross-check before quoting. Pre-submission verification for this paper compared the case-study week against the definitive indices (GFZ Kp; DRAO/Penticton F10.7 via NOAA's own feed archive). Kp and Dst matched throughout, but the dashboard's live F10.7 feed — which interleaves thrice-daily observations with forward-looking entries — displayed values up to ~215 sfu mid-week, while the definitive observed flux rose only from 94 to 117 sfu. The drag model's arithmetic was unaffected (it maps whatever it is fed, and the displayed values are reported as such in Section VII), but absolute flux values quoted from a live feed deserve a cross-check against definitive indices before entering a permanent record. A parser revision restricting the dashboard to observed noon values is queued for the next dashboard release.

IX. Limitations and Future Work

Intended use — Space Mission Control is intended for education, public-data exploration, and preliminary situational awareness. It is not an operational space-flight-safety, conjunction-assessment, orbit-determination, or re-entry-prediction system.

The density model is an empirical illustrative construct, not a certified atmospheric model; re-entry bands are coarse altitude heuristics; the tracker's sample is 670 of ~30,000 catalogued objects, so "nothing nearby" means nothing tracked nearby; the narrative engines are rule-based; and, as Section VIII (item 7) documents, live feed values can differ from definitive indices. A planned upgrade replaces the rule engines with calls to a multimodal vision-language-model endpoint (the panels already render that output shape). A second, deliberately separate future project addresses predictive debris early-warning — flagging active satellites that are beginning to fail (tumbling, fading beacons) from crowdsourced radio observations before catalogue reclassification — which requires a backend ingestion pipeline, authenticated data sources, and machine-learning infrastructure incompatible with this suite's zero-backend constraint.

X. Conclusion

Space Mission Control demonstrates that the full Sun-to-satellite causal chain can be made readable by non-specialists with public data, a browser, and no infrastructure. Its contribution is less any single algorithm than a set of working patterns: zero-backend resilience with honest degradation, rule-based translation standing in for LLM output, provider-respectful data citizenship, and story-ordered presentation. The suite is deployed as a static site; source and documentation are available under the MIT licence.

Acknowledgment

The author thanks the operators of NOAA SWPC, NASA SDO, and CelesTrak for maintaining open public data services, and the GFZ Helmholtz Centre and WDC for Geomagnetism (Kyoto) for the definitive indices used in pre-submission verification.

Disclosure of AI Assistance

This system was designed and implemented with AI assistance (Kimi AI, Moonshot AI) acting as a pair-programming and drafting tool under continuous human direction. All engineering decisions, data-validation steps, and the final text of this manuscript were reviewed, tested, and approved by the human author, who takes full responsibility for the content.

Data and Code Availability

Source code, documentation (user/developer manual and beginner's guide), and all figures in this paper are released under the MIT licence and archived on Zenodo: https://doi.org/10.5281/zenodo.21965564 (release v1.0.2, the exact version described in this manuscript; the concept DOI https://doi.org/10.5281/zenodo.21965563 always resolves to the latest release). The working repository is github.com/drngkwphilip/space-mission-control, and the live demonstration is at https://space-mission-control-2026.netlify.app. Data: NOAA SWPC [1], NASA SDO [5], CelesTrak [2].

References

[1] NOAA Space Weather Prediction Center, "Products and Data Services," https://services.swpc.noaa.gov (Kp, F10.7, Dst, solar wind, alerts, scales), accessed Aug. 15, 2026.

[2] T. S. Kelso, CelesTrak, https://celestrak.org; "A New Way to Obtain GP Data," CelesTrak documentation (gp.php API), 2026 revision, accessed Aug. 15, 2026.

[3] D. A. Vallado, P. Crawford, R. Hujsak, and T. S. Kelso, "Revisiting Spacetrack Report #3," in Proc. AIAA/AAS Astrodynamics Specialist Conf., Keystone, CO, USA, 2006, paper AIAA 2006-6753, doi: 10.2514/6.2006-6753.

[4] F. R. Hoots and R. L. Roehrich, "Models for Propagation of NORAD Element Sets," Spacetrack Report No. 3, U.S. Air Force Aerospace Defense Command, Colorado Springs, CO, USA, 1980.

[5] W. D. Pesnell, B. J. Thompson, and P. C. Chamberlin, "The Solar Dynamics Observatory (SDO)," Solar Physics, vol. 275, no. 1–2, pp. 3–15, 2012, doi: 10.1007/s11207-011-9841-3.

[6] J. M. Picone, A. E. Hedin, D. P. Drob, and A. C. Aikin, "NRLMSISE-00 empirical model of the atmosphere: Statistical comparisons and scientific issues," Journal of Geophysical Research, vol. 107, no. A12, 2002, doi: 10.1029/2002JA009430.

[7] D. Shashwat et al., satellite.js: SGP4/SDP4 propagation in JavaScript, v4.1.3, https://github.com/shashwatak/satellite-js, accessed Aug. 15, 2026.

[8] NOAA SWPC, "NOAA Space Weather Scales," https://www.swpc.noaa.gov/noaa-scales-explanation, accessed Aug. 15, 2026.

[9] Space-Track.org, U.S. Space Command public satellite catalogue, https://www.space-track.org (account required), accessed Aug. 15, 2026.

[10] Chart.js: open-source JavaScript charting library, v4.4.3, https://www.chartjs.org, accessed Aug. 15, 2026.

[11] J. Matzka, C. Stolle, Y. Yamazaki, O. Bronkalla, and A. Morschhauser, "The geomagnetic Kp index and derived indices of geomagnetic activity," Space Weather, vol. 19, 2021, doi: 10.1029/2020SW002641; Kp/ap data: GFZ Data Services, doi: 10.5880/Kp.0001.

[12] K. F. Tapping, "The 10.7 cm solar radio flux (F10.7)," Space Weather, vol. 11, pp. 394–406, 2013, doi: 10.1002/swe.20064; WDC for Geomagnetism, Kyoto, real-time Dst index, wdc.kugi.kyoto-u.ac.jp, accessed Aug. 16, 2026.